CHAPTER THREE:

IMAGING N-TYPE VOLTAGE-GATED CALCIUM CHANNEL PATTERNING

3.1 Introduction

Exocytosis is an important process in cell communication. Secretory vesicles are released after the arrival of a calcium-ion signal[38]. The probability of the exocytosis is thought to increase with the amount of proximal calcium channels[36]. Resolving the distribution of calcium channels at the cell membrane is therefore crucial for better understanding the exocytosis processes. Existing research has established that voltage-gated calcium channels are organised in clusters[71], but channel number, density and distribution has not been yet well explored.

The aim in this chapter is to investigate N-type calcium channel distribution at the plasma membrane. It is hypothesised that the total number of endogenous voltage gated calcium channels that can be quantified using TIRF microscopy. The number of channels in cells is likely to be higher for transfected calcium channels in HEK293 or PC12 cells.

I discuss whether the putative syntaxin-1A interaction site influences N-type calcium channel molecular organisation in the membrane. I also describe a novel method using pharmacological properties of ω-conotoxin[86], a high-affinity N-type calcium channel blocker, that allows for single-molecule-resolution imaging of endogenous calcium channels.

3.2 Localisation of N-type calcium channels

The membrane localisation of N-type calcium channels was verified by dual-colour colocalization microscopy of N-type calcium channels and syntaxin-1A. Cav2.2 calcium channels were expressed fused to EGFP in PC12 cells immunolabelled with anti-syntaxin-1A. 3D stacks were imaged using the Leica SP5 single molecule detection (SMD) confocal laser scanning microscope. Deconvolved images were analysed using Manders correlation coefficient[156] that measures the proportion of overlap pixels of each channel with the other. This coefficient is well-suited for analysis even when intensity signals from two proteins strongly differ[156]. Cav2.2-EGFP was selected as a channel 1 and syntaxin-1A-AlexaFluor658 as channel 2. The results of Manders correlation coefficient for a whole cell is represented in Figure 3.1a-c. The scatter plot represents the number of pixels of the EGFP and Alexa Fluor 658 intensities. The brighter the colour, the more pixels have those two intensity values for their two-colour channels[156]. The calculated means of the Manders

coefficient for the pixels above the channel 1 (tM1) and channel 2 (tM2) thresholds are 0.896 (±0.125 SD, n=5) and 0.856 (±0.169 SD, n=5) respectively. The high colocalization of N-type calcium channels with syntaxin-1A for a whole cell demonstrates the membrane localisation of transfected calcium channels. As a result of non-specific background which exist in every microscopy image, the result can be incorrect. The background for both channels has similar values of pixel intensities, which results in strong correlation. To overcome this problem the region of interest was chosen (figure 3.1d-f). The calculated means of the Manders coefficient for the pixels above the channel 1 (tM1) and channel 2 (tM2) thresholds are 0.722 (±0.356 SD, n=5) and 0.620 (±0.459 SD, n=5) respectively. There is colocalisation indicated for the regions of interest.

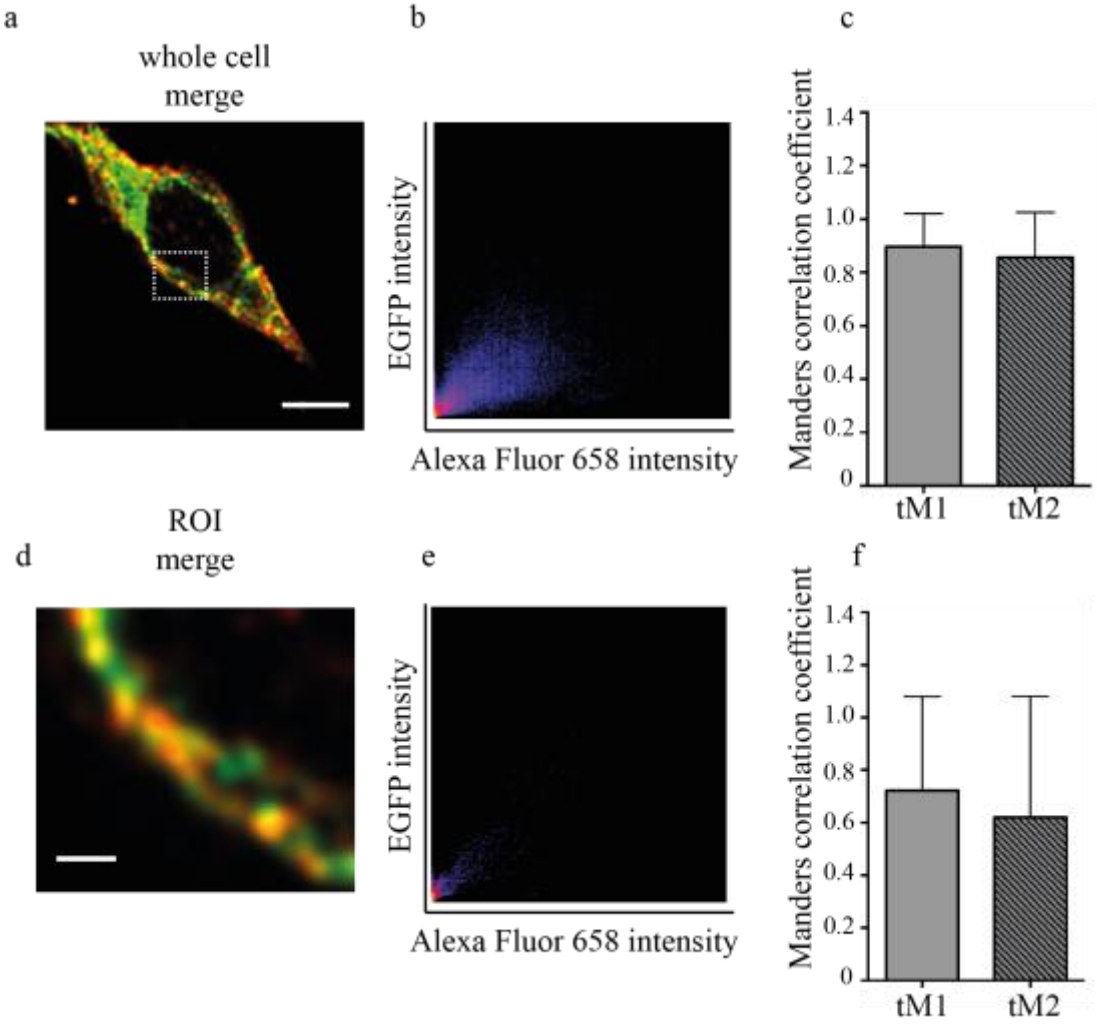

Figure 3.1 Manders correlation coefficient for Cav2.2-EGFP and syntaxin-1A AlexaFluor658. The N-type calcium channels (green) were expressed in PC12 cells and immunolabelled endogenous syntaxin-1A-AlexaFluor658 (red). Images were deconvolved and analysed with Manders' correlation coefficient. (a) Merged confocal image of the representative cell labelled with Cav2.2 - EGFP and syntaxin-1A - Alexafluor658. Scale bar 5 µm. (b) A frequency scatter plot of the pixel intensities of image (a) (c) Manders correlation coefficient. The graph represents the proportion of Cav2.2 overlap with syntaxin-1A 0.896 (±0.125 SD) (tM1) and proportion of syntaxin-1A overlap with Cav2.2 0.856 (±0.169 SD) (tM2) (number of cells=5). (d) Merged confocal image of the representative ROI indicated in (a). Scale bar 1µm. (e) A frequency scatter plot of the pixel intensities of image (d). (f) Manders correlation coefficient. The graph represents the proportion of Cav2.2 overlap with syntaxin-1A 0.722 (±0.356 SD) (tM1) and proportion of syntaxin-1A overlap with Cav2.2 0.620 (±0.459 SD) (tM2) (number of ROIs=5).

3.3 Distribution of N-type calcium channels using gated-STED microscopy

To check the overall spatial distribution of N-type calcium channels with 10s of nanometre certainty, time gated-stimulated emission depletion (gSTED)[107] was used. To visualize better and localize the calcium channels at the membrane, sheets of cell plasma membrane were made (Chapter 2.3.5). Cav2.2-EGFP calcium channels were expressed in HEK293 cells. Deconvolved CLSM and gSTED images were analysed. The FWHM of different spots was measured for gSTED images (Figure 3.2). The size of spots varies between 92.10 and 309.10 nm (median 156.4 nm) (Figure 3.2b). Regarding to the resolution limit of the STED microscope which is about 50 nm[105], it can be assumed that the N-type calcium channels are patterned in clusters.

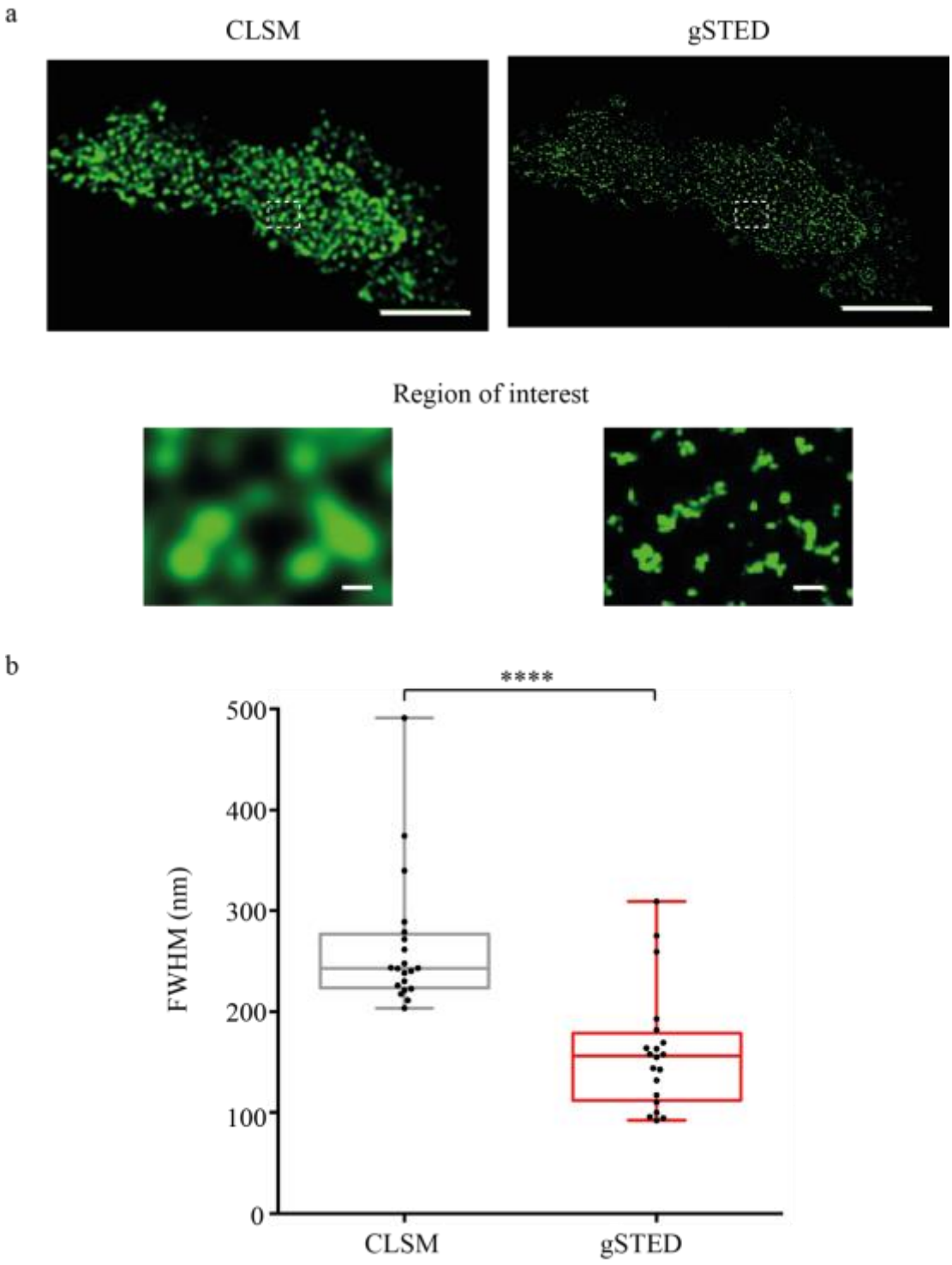

Figure 3.2 N-type calcium channel distribution in HEK293 cells plasma membrane sheets. (a) CLSM and gated-STED images of N-type calcium channels expressed with EGFP. Scale bar 5 µm (ROIs scale bar 1µm). (b) Boxplots of the FWHM cluster size (nm). (n of clusters= 10). The centre line indicates median value, the boxes 25th and 75th quartile values, and whiskers minimum and maximum values. Cell number = 4

3.4 Single molecule distribution of N-type calcium channels

To further understand N-type calcium channel molecular distribution, single molecule localisation microscopy was used. Cav2.2 calcium channels were expressed fused to photoactivatable mCherry (PAmCherry) in both PC12 and HEK293 cells. Fixed cells were imaged with Olympus IX-81 in TIRF mode. For this experiment, two variants of the CaV2.2-α_{1B} construct were used. Full-length PAmCherry-C1- CaV2.2-α_{1B} and the splice variant PAmCherry-C1- CaV2.2-α_{1B} [Δ18a] with deletion of exon 18a, that encodes the synaptic protein interaction site (synprint site)[28]. To date, it is believed that interaction of syntaxin-1A with N-type calcium channels through the synprint site is necessary for fast and effective exocytosis[28].

The series of PALM images were analysed in ThunderSTORM[157] Fiji plugin to report the localisation of each molecule (Figure 3.3a). The detected calcium channel psf signals were analysed and compared between the two variants (Figure 3.3b). The number of expressed N-type calcium channels detected in the same size region of interest inside of the cells was compared using the non-parametric Mann-Whitney U test. The box-and-whisker plots of the detection numbers for HEK293 and PC12 cells are presented in Figure 3.3b. The centre line indicates median value, the boxes 25^{th} and 75^{th} quartile values, and whiskers minimum and maximum values. The median number of the full-length Cav2.2 expressed in HEK293 cells is 31,304 while the splice variant Cav2.2(Δ18a) is smaller, 13,588 (Figure 3.3b). There is the significant difference between two variants expressed in HEK293 cells. A similar trend occurs for the number of expressed Cav2.2 calcium channels in PC12 cells. The median number of the full-length variant is 25,815 and for splice variant, Cav2.2(Δ18a) is 19,386. The statistical test determined no significant difference in the number of detected N-type calcium between Cav2.2 and Cav2.2(Δ18a) (Figure 3.3b). There is no significant difference in the number of expressed N-type calcium channels between HEK293 and PC12 cells.

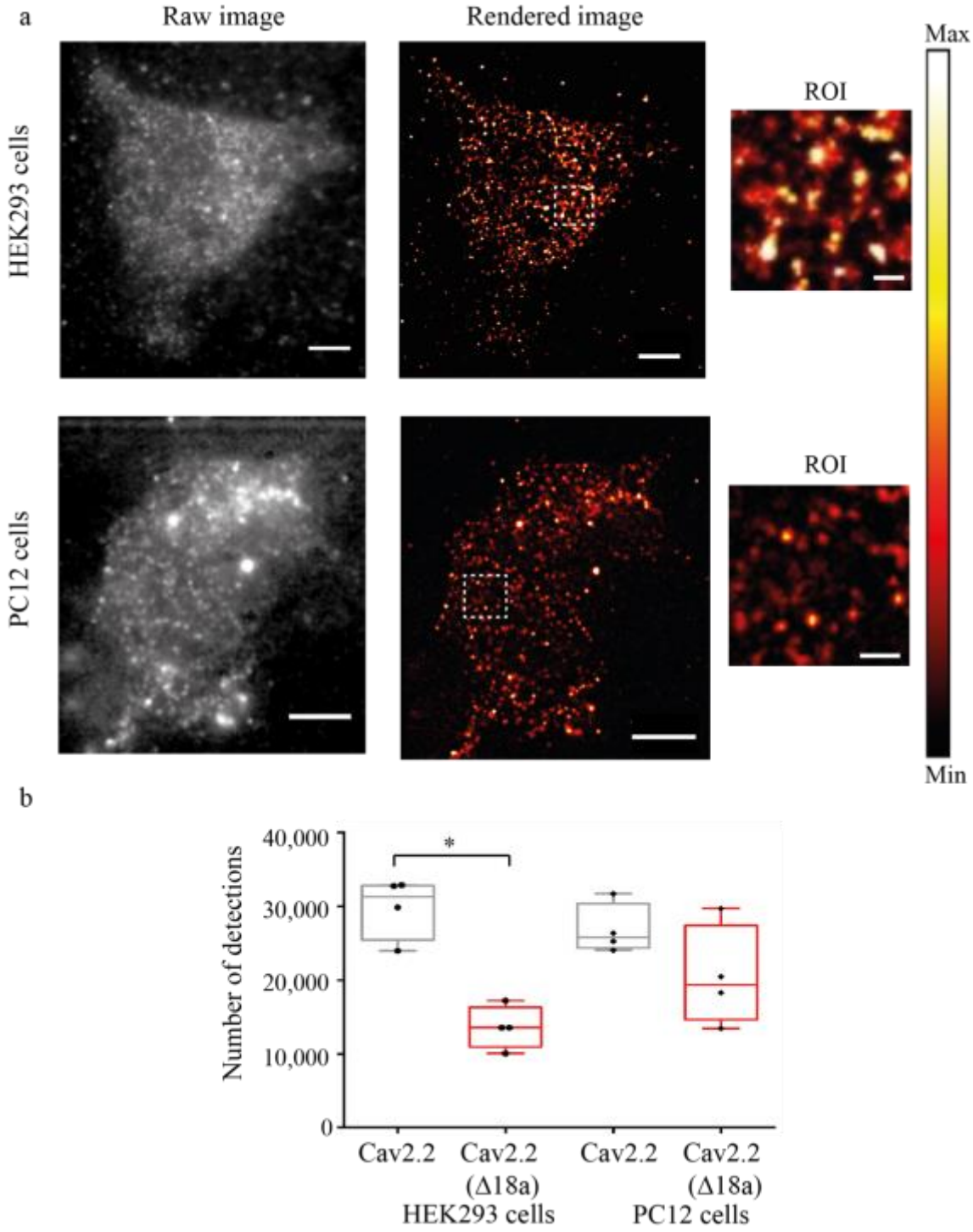

Figure 3.3 Distribution of the N-type calcium channels using PALM microscopy. (a) TIRF images of expressed Cav2.2-PACherry in HEK293 and PC12 representative cells. Raw images generated from a summation of all detected signals and rendered PALM images in ThunderSTORM plugin (scale 5 µm) (ROIs scale bar 1 µm). (b) Boxplots of the number of detections for two variants (Cav2.2 and with synprint site deletion Cav2.2(Δ18a) for ROIs inside of the HEK293 and PC12 cells. Statistical significance was verified using the non-parametric Mann-Whitney U test. N number of cells for each group =4.

3.4.1 N-type calcium channels cluster analysis

The x, y coordinates of localised psf were used to analyse the pattern of N-type calcium channel molecular distribution. Firstly, images were examined with Ripley's K function and its transformed L-function[158] (Chapter 2.6.4). The L-function value is larger than expected (above 0) in a short distance, which indicates the cluster pattering of N-type calcium channels (Figure 3.4a). To look in more detail at the clusters, Bayesian analysis[159] was used (Chapter 2.6.4). In the Figure 3.4b shows representative regions of interest for each variant expressed in HEK293 and PC12 cells. The maps of localised clusters are presented with a different colour for each cluster.

The median number of clusters of the full-length Cav2.2 in HEK293 cells is 331 clusters per cell, and for the Cav2.2(Δ18a) is 405 clusters (assuming the HEK293 cell surface ~177 μm^2)[200]. The percentage of molecules that are in clusters for both splice variants is 39-43%.

The radii of clusters and number of molecules per cluster were compared using the non-parametric Mann-Whitney U test. There is a significant difference between size of clusters in HEK293 cells. The median number of the full-length variant is 42.24 nm and for the splice variant is 31.24 nm (Figure 3.4c). The difference in number of molecules within each cluster is also significantly different (Figure 3.4c), with the median number of molecules per cluster for Cav2.2 69 and for the Cav2.2(Δ18a) two times smaller at 35.

The clusters of expressed N-type calcium channels in PC12 cells, were analysed using the same method. The median number of clusters for the full-length Cav2.2 variant is 249 clusters per cell, and for the splice variant Cav2.2(Δ18a) is 230 clusters (assuming the PC12 cell surface ~133 μm^2)[200]. The percentage of molecules organised in clusters is 34-36%. The radii of clusters were compared using the non-parametric Mann-Whitney U test. There is a significant difference between the size of clusters in PC12 cells, with the median number of the full-length Cav2.2 37.38 nm and for the splice variant Cav2.2(Δ18a) 32.26 nm (Figure 3.4c). There is a significant difference in number of molecules within each cluster (Figure 3.4c). The median number of molecules in the Cav2.2 clusters is 66 and for the Cav2.2(Δ18a) is 40. Statistical tests showed no significant difference in clusters between HEK293 and PC12 cells.

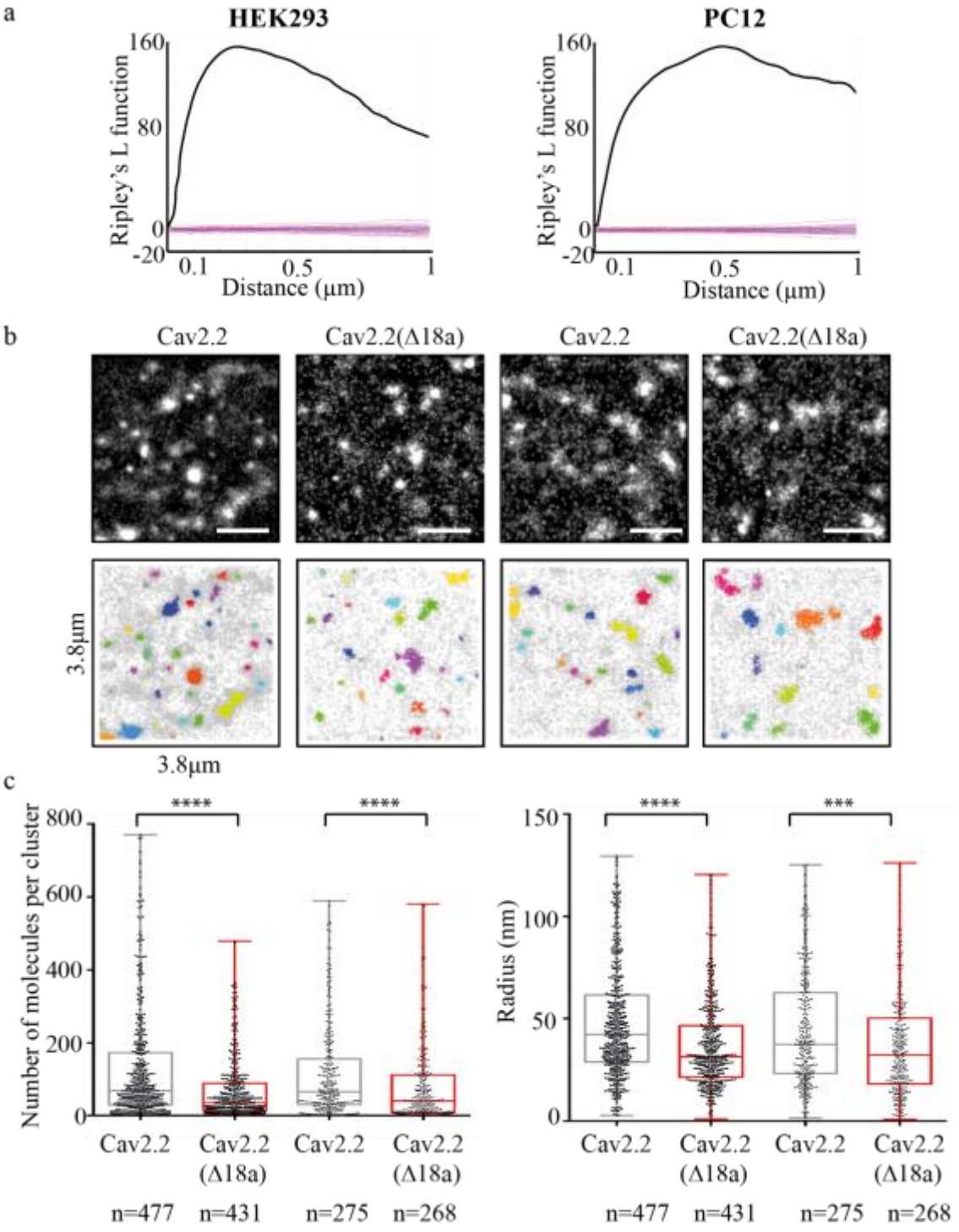

Figure 3.4 N-type calcium channel clusters analysis. (a) The deviation of Ripley's L function from 0 indicates the cluster distribution. (b) The rendered images of ROIs for representative cells for each variant are presented (scale bars 1 µm). The maps of localised clusters using Bayesian analysis are presented. Different colour represents each cluster. (c) Boxplots of number of molecules in each cluster and radius of clusters for HEK293 and PC12 cells. Statistical significance was verified using the non-parametric Mann-Whitney U test. Number of cells for each group =4. n represents number of clusters.

3.5 Endogenous N-type calcium channels labelling with ω-conotoxin-Cage552

The techniques described above allow the study of heterologous exogenous N-type calcium channels. A big advantage would be to analyse the distribution of *endogenous* N-type calcium channels. One of the tools that I would like to describe is a novel staining method using the pharmacological properties of the ω-conotoxin GVIA. As described in Chapter 1.3, ω-conotoxin GVIA blocks the N-type calcium channels with high specificity[85]. I hypothesised that the toxin, conjugated to the Cage552 fluorescent dye (1:1) can detect single N-type calcium channels.

Firstly, the principle of the fluorescent dye uncaging was tested by attaching with Cell-Tak ω-conotoxin-Cage552 to the glass coverslip. Cage552 fluorescent dye was photoactivated with 405 nm laser pulses followed by imaging with 561 nm laser in TIRF mode (60 ms frame rate). Molecules were emitting fluorescence for only a few frames and then they photobleached irreversibly (Figure 3.5b). Comparison to Alexa Fluor 647 fluorescent dye was made. Alexa Fluor 647 is commonly used as a secondary antibody that detects the primary antibody. The Alexa Fluor 647 switched repeatedly between an active and no in active fluorescent state, in contrast to the single emission period of Cage552 dye (Figure 3.5c). Additionally, the labelling with the secondary antibody can lead to multiple labelling and multiple detections of the same target molecule. That is because the multiple molecules of the secondary antibody can be attached to the one specific, primary antibody, results in several fluorescent dyes attached to one target protein[218].

The Cav2.2 calcium channels were expressed fused to EGFP in HEK293 cells. Following the protocol described in Chapter 2.5.7, cells were imaged using Olympus XI-81 in TIRF mode. As a result of positively charged ω-conotoxin molecules, the toxin sticks to coverslip outside of the cells, causing the high level of the background (Figure 3.6). The experiments were repeated with lower concentrations of labelled ω-conotoxin (0.5 nM to 0.5 µM) (Figure 3.6). The non-transfected PC12 cells differentiated with nerve growth factor β[150] (Chapter 2.1.3) were also tested with different concentration of ω-conotoxin-Cage552. Various concentrations of BSA/FSG/peptone blocker were used. To overcome the background staining problem, scrambled ω-conotoxin was also tested, added to the cells for 30 min before imaging as a blocker. The examined procedures did not give positive results. The ω-conotoxin concentration below 0.1 µM has 0% blocking potency (Figure 2.3

Chapter 2.6.7) and for higher concentrations, the background cannot be eliminated (Figure 3.6).

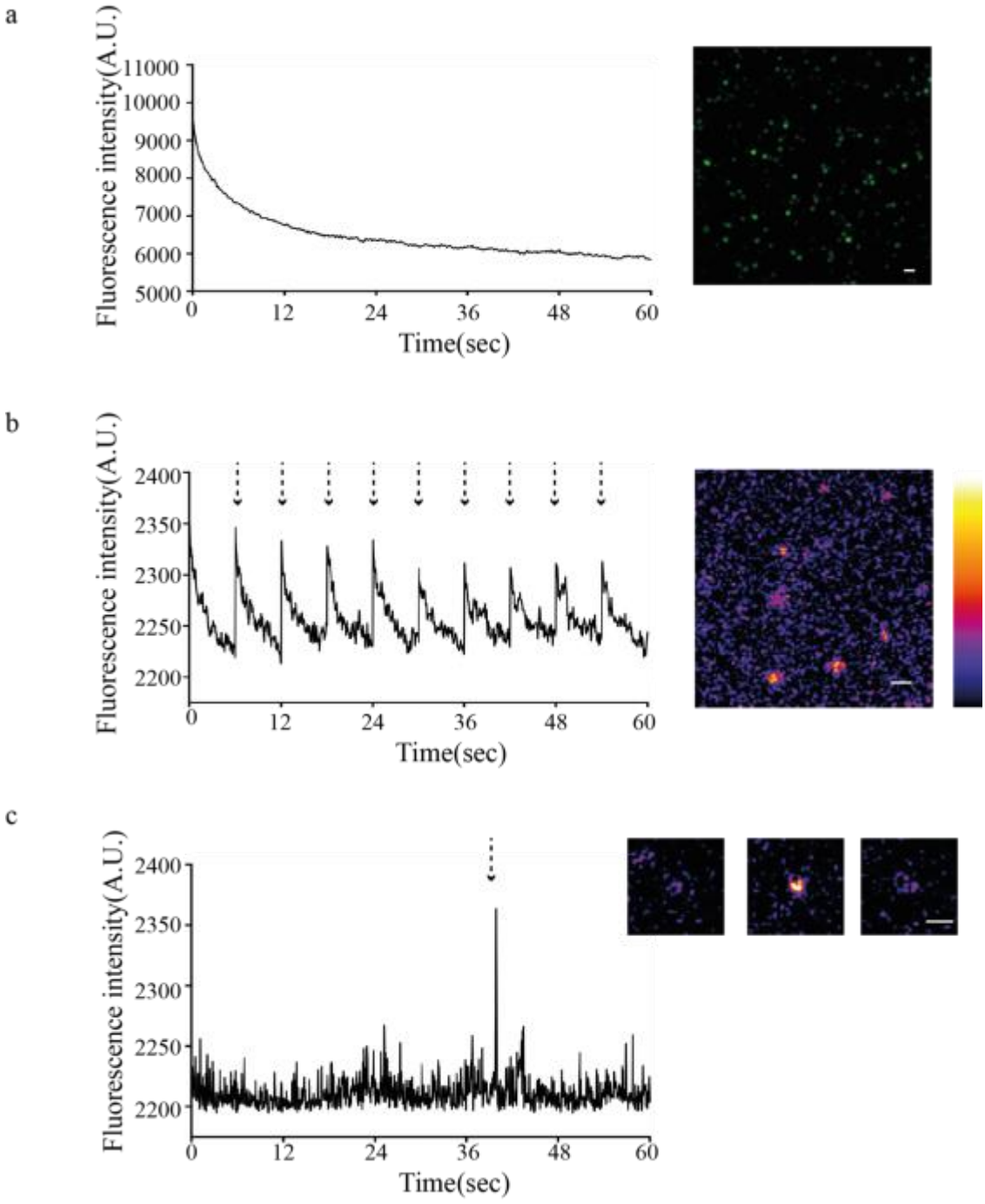

Figure 3.5 Principles of the ω-conotoxin-Cage552. (a) Fluorescence intensity changes of attached molecules of Alexa Fluor 647 to the coverslip and imaged in TIRF mode. (b) Fluorescence intensity changes of attached molecules of the ω-conotoxin-Cage552 to the coverslip and imaged in TIRF mode. (c) Fluorescence intensity profile of ω-conotoxin-Cage552single molecule. Arrows indicate excitation with 405 nm laser. Scale bar 1 µm.

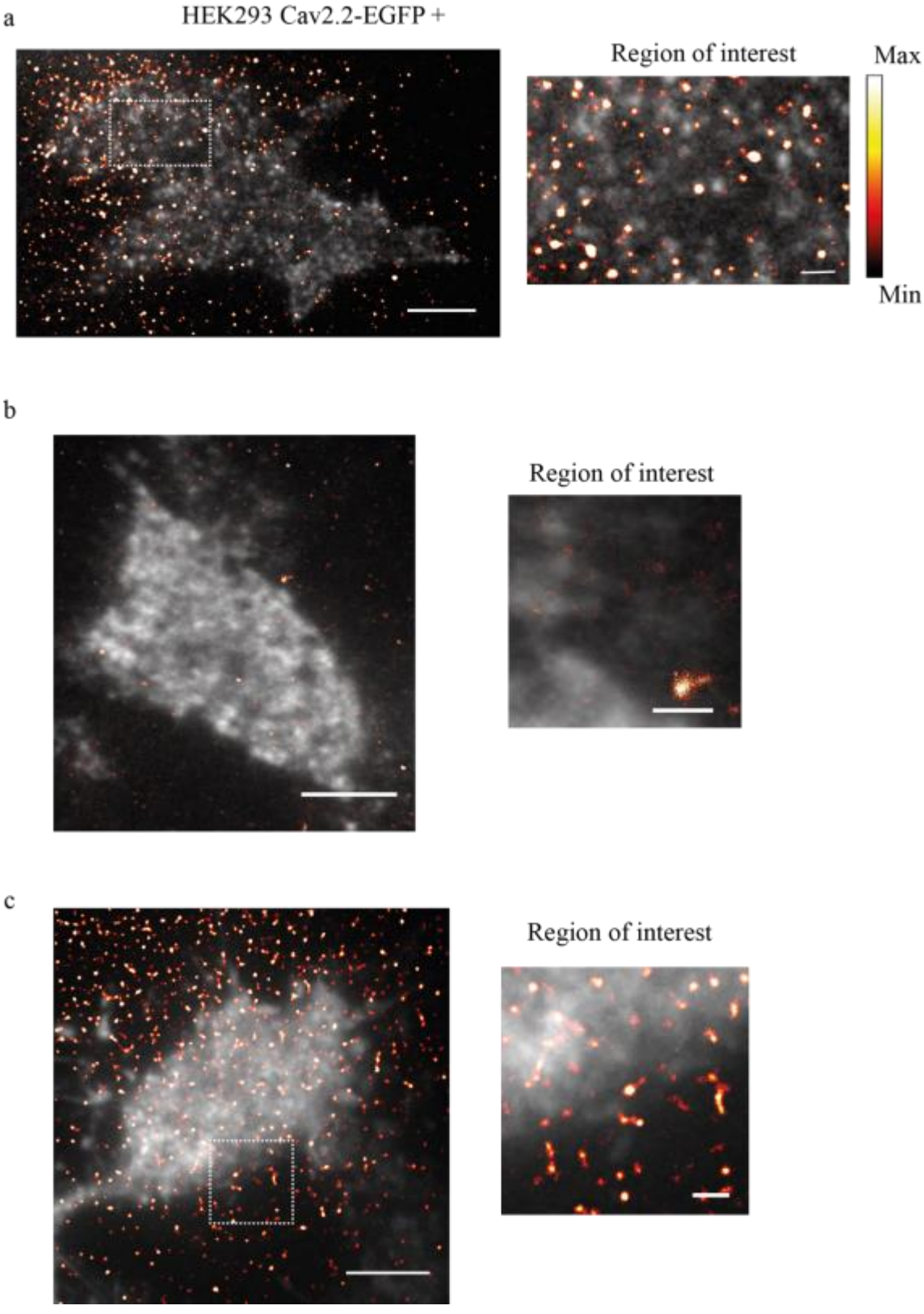
a
HEK293 Cav2.2-EGFP +
Region of interest
Max
Min
b
Region of interest
c
Region of interest

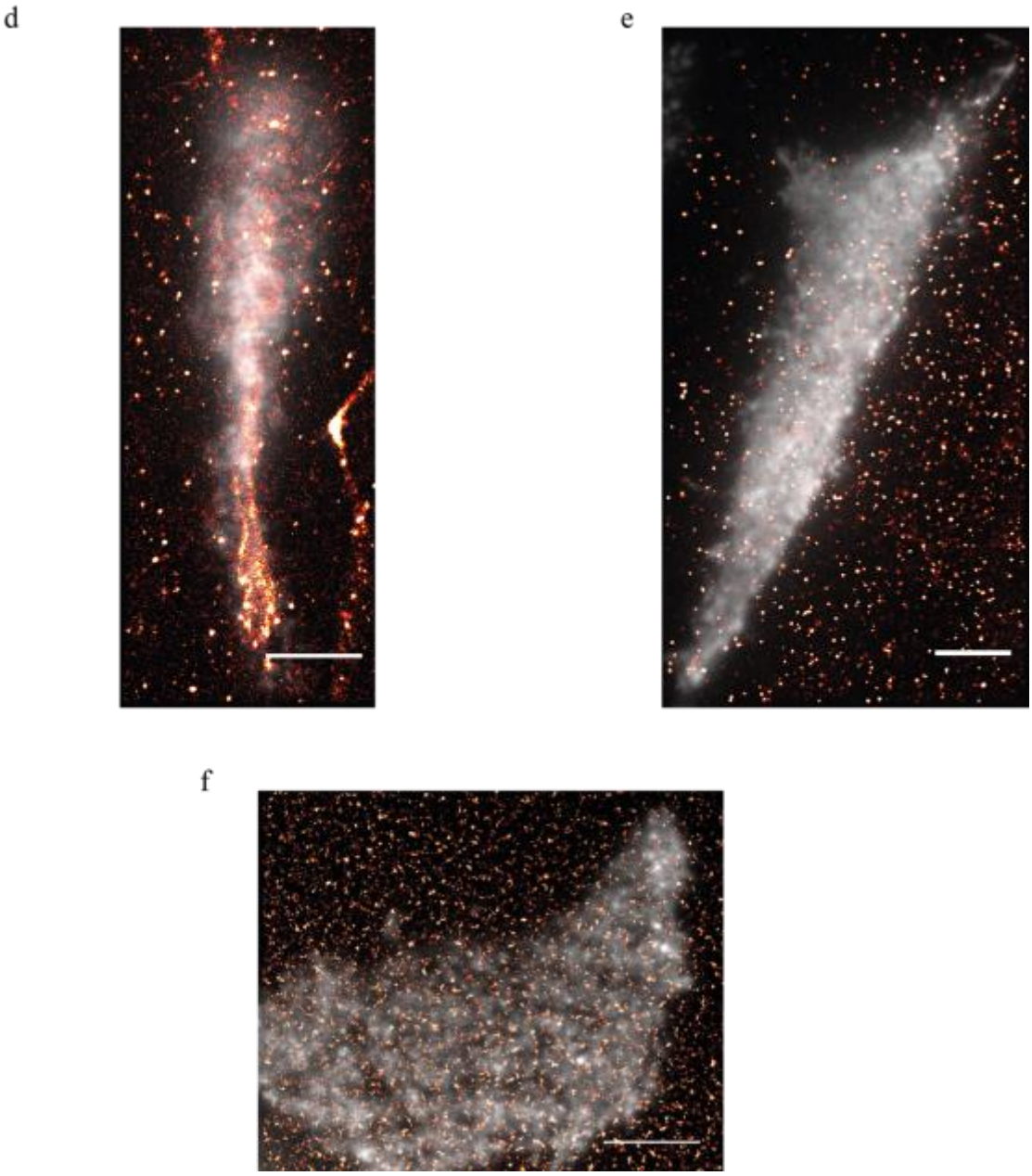

Figure 3.6 ω-conotoxin-Cage552 labelling of N-type calcium channels in live cells. TIRF images of (a) HEK293 cell transfected with Cav2.2-EGFP(grey), BSA/FSG blocking, 0.5 µM ω-conotoxin-Cage552 (red hot). (b) HEK293 cell transfected with Cav2.2-EGFP (grey), BSA/FSG blocking, 0.5 nM ω-conotoxin-Cage552 (red hot). (c) HEK293 cell transfected with Cav2.2-EGFP (grey), BSA/FSG blocking, 0.2 µM ω-conotoxin-Cage552 (red hot). (d) HEK293 cell transfected with Cav2.2-EGFP (grey), higher concentration BSA/FSG blocking, 0.5 µM ω-conotoxin-Cage552 (red hot). (e) AtT20 cell transfected with SNAP25-EGFP (grey). BSA/FSG blocking, 0.5 µM ω-conotoxin-Cage552 (red hot). Scale bar 5 µm (ROIs 1 µm). (f) HEK293 cell transfected with Cav2.2-EGFP (grey), scrambled ω-conotoxin blocking, 0.5 µM ω-conotoxin-Cage552 (red hot). Scale bars 5 µm (ROIs 1 µm).

3.6 Conclusions

Due to the limit of the spatial resolution, the nanoscale distribution of voltage-gated calcium channels has not been well explored. The experimental evidence suggests that calcium channels form clusters at the cell membrane[71,203] where vesicles are docked and released. It is proposed that vesicle docking and fusion take place through the syntaxin-1A and synaptic protein interaction site located at the main subunit of N-type calcium channels[46]. The aim of this chapter was to understand better N-type calcium channels distribution and examine the influence of the synprint site on their pattering.

Firstly, the membrane localisation of expressed N-type calcium channels was confirmed. The Manders correlation coefficient was used to measure the proportion of overlapping the N-type calcium channels with syntaxin-1A. The results for the whole cell colocalisation presented in Figure 3.1a-c suggest a high localisation of N-type calcium channels at the cell membrane in PC12 cells. The N-type calcium channels expressed with EGFP colocalized with labelled endogenous syntaxin-1A with coefficient 0.896 (±0.125 SD n=5) (Figure 3.1c). However, the non-specific background may exert an influence on this high colocalization, the regions of interest were analysed for each cell. After calculation the Manders coefficient, there is colocalization between N-type calcium channels and syntaxin-1A (0.722 (±0.356 SD, n=5) figure 3.1d-f).

To check the overall distribution of N-type calcium channels and verify their cluster conformation, the gated-STED technique was used. HEK293 cells with expressed Cav2.2-EGFP calcium channels were unroofed with sonic waves to create the plasma membrane sheets. The analysis of FWHM of measured spots size revealed the size between 100 and 300nm. The results can be considered as clusters pattering of N-type calcium channels regarding to the gSTED resolution limit which is around 50 nm[105].

To analyse the N-type calcium channel distribution at the single molecule level PALM was used. Results presented in Figure 3.3 show the number of expressed molecules in two different cell types. The studies on HEK293 cells indicate expression of endogenous calcium channels but no expression of syntaxin-1A or SNAP-25. These calcium channels have some similarities with R-type high-voltage gated calcium channels or T-type low-voltage gated calcium channels[204]. PC12 cells mainly express L-type calcium channels[205]. The number of localised molecules in HEK293 and PC12 cells indicates high expression

levels of N-type calcium channels (Figure 3.3). There is lower expression number of splice variant (Cav2.2(Δ18a) for both cell types. There is no significant difference of a number of localised molecules between two cell types, but there is a significant difference (p=0.0286) between two variants expressed in HEK293 cells. These results can be interpreted in two different ways. First, that there is a tendency to express fewer molecules for Cav2.2(Δ18a) variant which is not related to the syntaxin-1A occurrence. The second conclusion is that in the cells without endogenous SNARE proteins this tendency is much higher and has a significant influence on the lower expression of N-type calcium channels without the synaptic protein interaction site.
The cluster results from gSTED indicated the cluster patterning were verified with Ripley's K function analysis. Individual clusters were analysed with more detail using Bayesian analysis and compared between two variants (Figure 3.4) of N-type calcium channels expressed in HEK293 and PC12 cells. The results from HEK293 cells expressing splice N-type calcium channels (Cav2.2Δ18a) showed lower expression of molecules than for full-length variant. Although the number of clusters is higher, they are smaller in number of molecules and radii size.

The results show the significant difference between full-length and splice variant in a number of molecules per cluster and cluster size for both cell types. The sizes of clusters and number of N-type calcium channels in variant without the synprint motif is smaller.
It can be concluded that the channels without synprint motif, that cannot interact with SNARE proteins, form clusters with fewer molecules number and smaller radii size.

Previous research[206] indicated that the expression of N-type calcium channels at the presynaptic terminals, lacking the synprint site is reduced. They also indicate the lower clustered in the nerve terminals[206]. The research on invertebrates demonstrated[207] that the lack of synaptic interaction site has no influence on neurotransmitter release.

My results together with previous research indicate the role of the synprint site in the N-type calcium channels distribution. As suggested in previous studies the synprint site is an important role in interaction with membrane SNARE proteins which is necessary for exocytosis machinery[27,45]. The interaction with Syntaxin-1A and influence on N-type calcium channel behaviour I will discuss in chapter four.

The overexpression of exogenous N-type calcium channels can have an influence on results of distribution and size of clusters. As presented on boxplots in figure 3.4 the number of molecules per cluster vary between cells and Cav2.2 calcium channel variants.

A photoactivatable fluorescent protein like PACherry has a size of 4 nm[208] and is linked to the protein of interest, here CaV2.2-α1B, by the linker of length around 5 nm[208]. This can lead to errors for example in cluster size. To overcome this problem the novel staining methods with N-type calcium channel specific ω-conotoxin GVIA was proposed. The advantage of ω-conotoxin is blocking the N-type calcium channels in the ratio 1:1[85]. Conjugated one molecule of conotoxin to one molecule of Cage552 fluorescent dye is a highly specific method for endogenous N-type calcium channels labelling. Although the labelled ω-conotoxin still blocks the N-type calcium channels, the three times higher concentration than for unlabelled ω-conotoxin is needed (Figure 2.3). The disadvantage of the ω-conotoxin-Cage552 is its sticky nature. As a result, the high background outside of the cell was imaged. It is hard to estimate if the imaged signal identifies the blocked calcium channels or randomly attached molecule to the cell. This method is a promising tool for single molecule imaging of endogenous N-type calcium channels but still has to be improved to avoid attaching molecules to the coverslip and to be able to indicate only blocked channels.